# Intramolecular Exciplex and Intermolecular Excimer Formation of 1,8-Naphthalimide−Linker−Phenothiazine Dyads

**Dae Won Cho,[†,§] Mamoru Fujitsuka,[†] Kyung Hwa Choi,[‡] Man Jae Park,[‡] Ung Chan Yoon,[‡] and Tetsuro Majima*[,†]**

*The Institute of Scientific and Industrial Research (SANKEN), Osaka University, Mihogaoka 8-1, Ibaraki, Osaka 567-0047, Japan, and Department of Chemistry and the Chemistry Institute for Functional Materials, Pusan National University, Pusan 609-735, Korea*

*Received: October 24, 2005; In Final Form: January 18, 2006*

Steady-state fluorescence spectra were measured for 1,8-naphthahlimide−linker−phenothiazine dyads (NI−L−PTZ, where L = octamethylenyl ($(CH_2)_8$) and 3,6,9-trioxaundecyl ($(CH_2CH_2O)_3C_2H_4$)), NI−C8−PTZ and NI−O−PTZ, as well as the NI derivatives substituted on the nitrogen atom with various linker groups without PTZ as the reference NI molecule in *n*-hexane. Normal fluorescence peaks were observed at 367−369 nm in all NI molecules together with a broader emission around 470 nm, which is assigned to the excimer emission between the NI in the singlet excited state ($^1$NI*) and the NI moiety of another NI molecule ($^1$[NI/NI]*). In addition, a broad peak around 600 nm was observed only for NI−L−PTZ, which is assigned to an intramolecular exciplex emission between donor (PTZ) and acceptor (NI) moieties in the excited singlet state, $^1$[NI−L−NI]*. The formation of an intramolecular exciplex corresponds to the existence of a conformer with a weak face-to-face interaction between the NI and PTZ moieties in the excited state because of the long and flexible linkers. The excited-state dynamics of the NI molecules in *n*-hexane were established by means of time-resolved fluorescence spectroscopy.

## 1. Introduction

Among various molecular interactions in the excited states, a photoinduced electron transfer (PET) is the most important in photophysical, photochemical, and photobiological reaction processes.[1−4] There are two kinds of PET processes. One is an intermolecular PET process between electron donor (D) and acceptor (A) molecules, leading to the formation of various ion radical pairs as well as subsequent chemical reactions. The other is an intramolecular PET process for D−A molecules bridged with various linkers (L), namely, dyad and triad systems, leading to the charge-separated state, $D^{\bullet+}-L-A^{\bullet-}$, which might lead to synthetically useful chemical reactions.[5]

The photophysical properties of various dyads and triads have been thoroughly investigated with respect to PET, because it resembles to the photosynthetic system. Various studies for the dyad and triads have reported that PET can take place very rapidly and efficiently.[6−8] Among the photophysical properties of the dyads, the mechanism and kinetics of PET and charge recombination have been extensively studied. The charge interaction between $D^{\bullet+}$ and $A^{\bullet-}$ of $D^{\bullet+}-L-A^{\bullet-}$ with various flexible linkers has been found to cause a radiative pathway through the formation of an intramolecular exciplex between D and A moieties ($^1$[D/A]*).[9−11]

The formation process of the intramolecular exciplex in D−L−A dyads with flexible linkers depends on the solvent polarity, because it affects the geometrical structure of $D^{\bullet+}-L-A^{\bullet-}$.[9] Mataga et al. have provided evidence supporting that the average DA distance of the polar exciplexes increases as the solvent polarity increases.[9] This evidence relates partly to intermolecular exciplexes[12] but mostly to intramolecular exciplexes formed in D−$(CH_2)_n$−A dyads, where D and A are linked by a flexible polymethylene chain.[12−17] In a number of D−$(CH_2)_n$−A dyads, the exciplex geometry is concluded to change from "compact" in nonpolar to "loose" in polar solvents. In other words, a fully folded and a more or less extended conformation of intramolecular exciplexes between D and A in D−$(CH_2)_n$−A dyads are considered to be dominant in nonpolar and polar solvents, respectively.

1,8-Naphthalimide (NI) derivatives have received considerable attention for both their spectroscopic properties and their potential applications in biology. Since these compounds have excellent electron-acceptor properties, they have been used in many studies of the PET involving NI and various donors.[18] They can intercalate into specific positions of DNA and can induce photocleavage of a DNA double helix.[19,20] We have recently reported that PET of NI-modified DNA follows by a charge-transfer process in DNA depending on the nucleobase sequences.[21] Because of those applications, the photophysical properties of NI molecules have been mostly studied in polar solvents such as acetonitirle or water but those in nonpolar solvents have not been thoroughly studied and reported.

In this study, we have studied the photophysical properties of 1,8-naphthalimide−linker−phenothiazine dyads, NI−C8−PTZ and NI−O−PTZ (NI−L−PTZ, where L = octamethylenyl ($(CH_2)_8$) and 3,6,9-trioxa-undecanyl ($(CH_2CH_2O)_3C_2H_4$), respectively), as well as the NI molecules substituted with various linker groups such as methyl, *n*-hexyl, 2-methoxyethyl, 2-methylthioethyl, 3,6,9-trioxaundecyl, and 3,9-dithio-6-oxa-undecyl, corresponding to NI−C1, NI−C7, NI−O1, NI−S, NI−O3, and NI−SOS, respectively, in *n*-hexane as shown in Scheme

* To whom correspondence should be addressed. E-mail: majima@sanken.osaka-u.ac.jp.
† Osaka University.
‡ Pusan National University.
§ Present address: Department of Chemistry, Chosun University, Gwangju 501-759, Korea.

10.1021/jp056078p CCC: $33.50 
Published on Web 02/14/2006

**SCHEME 1**

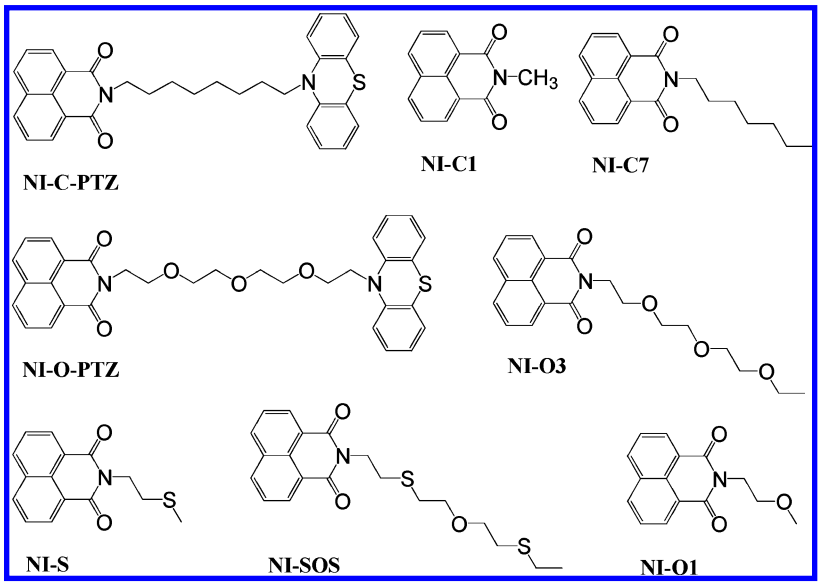


1. We have also carried out the time-resolved emission spectroscopic studies of NI−L−PTZ and NI−L in order to elucidate the excited-state dynamics.

## 2. Experimental Section

**Materials.** Syntheses of NI−L−PTZ and reference NI molecules were carried out as following.

***N*-(8-Phenothiazinyloctyl)-1,8-naphthalimide (NI−C−PTZ).** *N*-(8-Iodooctyl)-1,8-naphthalimide was synthesized from the reaction of 1,8-naphthalimide (4.9 g, 25 mmol), NaH (1 g, 25 mmol, 60% in mineral oil), and 1,8-diiodooctane (8.8 g, 25 mmol) in the similar manner for NI−C1 in a yield of 5.5 g (47%). $^1$H NMR ($CDCl_3$) 1.28 (s, 8H), 1.81 (m, 2H), 2.17 (m, 2H), 3.20 (t, 2H), 3.50 (t, 2H), 7.73 (t, 2H), 8.16 (d, 2H), 8.57 (d, 2H). $^{13}$C NMR ($CDCl_3$) 7.1, 27.6, 29.1, 30.1, 30.5, 30.6, 34.2, 42.3, 124.8, 127.9, 128.3, 132.2, 133.3, 134.9, 164.5. A solution mixture of phenothiazine (2.7 g, 13 mmol) and NaH (0.6 g, 15 mmol, 60% in mineral oil) in 30 mL of DMF was stirred for 2 h at 80 °C. *N*-(8-Iodooctyl)-1,8-naphthalimide (5.5 g, 13 mmol) was dropped to the solution for 30 min and stirred for 12 h at 100 °C. The resulting mixture was cooled, dried, and concentrated in vacuo to afford a residue which was purified by column chromatography to yield 5.0 g (78%) of NI−C8−PTZ as a viscous oil. $^1$H NMR ($CDCl_3$) 1.26 (m, 6H), 1.58 (m, 4H), 3.10 (t, 2H), 3.20 (t, 2H), 6.80−7.11 (m, 8H), 7.74 (t, 2H), 7.91 (d, 2H), 8.01 (d, 2H). $^{13}$C NMR ($CDCl_3$) 27.0, 27.1, 27.2, 28.3, 29.4, 29.5, 40.6, 47.6, 115.6, 122.5, 122.7, 124.9, 127.0, 127.4, 127.5, 128.1, 131.1, 131.5, 133.9, 145.4, 164.1. FAB-MS for NI−C−PTZ: found, 507.3 (calcd for [NI−C−PTZ + 1], 507.20).

***N*-(11-Phenothiazinyl-3,6,9-trioxaundecyl)-1,8-naphthalimide (NI−O−PTZ).** Tetraethylene glycol dimesylate ether was prepared from bismesylation of tetraethylene glycol by methanesulfonyl chloride and triethylamine. Two mesyloxy groups of tetraethylene glycol dimesyl ether were substituted by iodide using NaI to give tetraethylene glycol diiodide. *N*-(11-Iodo-3,6,9-trioxaundecyl)-1,8-naphthalimide was synthesized from the reaction of 1,8-naphthalimide (2.5 g, 12 mmol), NaH (0.6 g, 15 mmol, 60% in mineral oil), and tetraethylene glycol diiodide (5.0 g, 12 mmol) in 20 mL of DMF in a similar manner as that for NI−C1 in a yield of 4.3 g (74%). $^1$H NMR ($CDCl_3$) 3.22 (t, 2H), 3.56−3.61 (m, 10H), 3.66 (t, 2H), 3.97 (t, 2H), 7.72 (t, 2H), 8.06 (d, 2H), 8.34 (d, 2H). $^{13}$C NMR ($CDCl_3$) 14.3, 40.7, 69.5, 69.9, 71.0, 73.5, 122.5, 127.3, 131.7, 131.8, 134.5, 134.6, 164.3. NI−O−PTZ was synthesized from the reaction of phenothiazine (1.2 g, 6 mmol), NaH (0.3 g, 7 mmol, 60% in mineral oil), and *N*-(11-iodo-3,6,9-trioxaundecyl)-1,8-naphthalimide (3 g, 6 mmol) in 20 mL of DMF in a similar manner as that for NI−C1 in a yield of 1.8 g (55%) of NI−O−PTZ as a viscous oil. $^1$H NMR ($CDCl_3$) 3.51 (t, 2H), 3.55 (t, 2H), 3.60−3.70 (m, 8H), 3.83 (t, 2H), 4.01 (t, 2H), 6.83−6.87 (s, 8H), 7.08 (t, 2H), 8.14 (d, 2H), 8.55 (d, 2H). $^{13}$C NMR ($CDCl_3$) 39.6, 58.7, 68.5, 70.1, 115.7, 122.3, 122.4, 122.5, 122.9, 126.1, 127.1, 127.3, 127.6, 131.4, 131.8, 134.8, 164.5. FAB-MS for NI−O−PTZ: found, 555.4 (calcd for [NI−O−PTZ + 1], 555.19).

***N*-Methyl-1,8-naphthalimide (NI−C1).** A solution of 1,8-naphthalimide (4.9 g, 25 mmol) and NaH (1 g, 25 mmol, 60% in mineral oil) in 50 mL of DMF was stirred for 2 h at 80 °C. Iodomethane (3.5 g, 25 mmol) was slowly dropped to the solution for 30 min and stirred for 8 h at 80 °C. The resulting mixture was cooled, dried, and concentrated in vacuo to afford a residue which was subjected to recrystallization to yield 4.4 g (83%) of NI−C1. Mp 210−211 °C. $^1$H NMR ($CDCl_3$) 3.50 (s, 3H), 7.68 (t, 2H), 8.13 (d, 2H), 8.50 (d, 2H). $^{13}$C NMR ($CDCl_3$) 27.5, 127.1, 128.0, 131.3, 131.4, 133.8, 134.1, 164.8.

***N*-Heptyl-1,8-naphthalimide (NI−C7).** NI−C7 was synthesized from 1,8-naphthalimide (4.9 g, 25 mmol), NaH (1 g, 25 mmol, 60% in mineral oil), and 1-iodoheptane (5.7 g, 25 mmol) in a similar manner as that for NI−C1 in a yield of 4.3 g (58%). Mp 70−72 °C. $^1$H NMR ($CDCl_3$) 0.78 (t, 3H), 1.25 (m, 8H), 1.63 (m, 2H), 4.02 (t, 2H), 7.55 (t, 2H), 8.00 (d, 2H), 8.37 (d, 2H). $^{13}$C NMR ($CDCl_3$) 14.3, 22.8, 27.3, 28.3, 29.2, 32.0, 40.6, 122.7, 126.9, 128.0, 131.1, 131.5, 133.7, 164.0. FAB-MS for NI−C7: found, 296.8 (calcd for [NI−C7 + 1], 296.16).

***N*-(2-Methoxylethyl)naphthalimide (NI−O).** *N*-(2-Hydroxylethyl)-1,8-naphthalimide was prepared from the reaction of 1,8-naphthalimide and 2-bromoethanol in the presence of NaH. NI−O was synthesized from *N*-(2-hydroxylethyl)-1,8-naphthalimide (6.0 g, 25 mmol), Na (0.5 g, 21 mmol), and 1-iodomethane (3.5 g, 25 mmol) in 30 mL of THF in a similar manner as that for NI−C1 in a yield of 3.8 g (71%). Mp 115−117 °C. $^1$H NMR ($CDCl_3$) 3.38 (s, 3H), 3.73 (t, 2H), 4.44 (t, 2H), 7.74 (t, 2H), 8.20 (d, 2H), 8.59 (d, 2H). $^{13}$C NMR ($CDCl_3$) 39.3,

58.9, 69.8, 122.9, 126.9, 128.0, 131.1, 131.3, 133.9, 164.0. FAB-MS for NI−O: found, 256.6 (calcd for [NI−O + 1], 256.09).

***N*-(3,6,9-Trioxaundecyl)-1,8-naphthalimide (NI−O3).** A solution of 3,6-dioxa-octanol (2.1 g, 16 mmol) and Na (0.4 g, 25 mmol) in 30 mL of THF was stirred for 2 h at 50 °C. *N*-(2-bromoethyl)-1,8-naphthalimide (5 g, 16 mmol) was slowly added in a dropwise manner into the solution for 30 min and stirred for 10 h at 80 °C. The resulting mixture was cooled, dried, and concentrated in vacuo to afford a residue which was subjected to recrystallization to yield 4.0 g (64%) of NI−O3. Mp 192−195 °C. $^1$H NMR ($CDCl_3$) 1.25 (t, 3H), 4.08−4.18 (m, 8H), 4.26 (d, 2H), 4.32 (d, 2H), 4.67 (d, 2H), 7.65 (t, 2H), 8.10 (d, 2H), 8.43 (d, 2H). $^{13}$C NMR ($CDCl_3$) 1.3, 40.7, 41.4, 43.0, 62.0 (four $CH_2O$), 122.4, 127.2, 131.6, 131.7, 134.4, 134.5, 164.2. FAB-MS for NI−O3: found, 358.7 (calcd for [NI−O3 +1], 357.16).

***N*-(2-Methylthioethyl)-1,8-naphthalimide (NI−S).** A solution of 1,8-naphthalimide (5 g, 25 mmol) and NaH (1 g, 25 mmol, 60% in mineral oil) in 50 mL of DMF was stirred for 2 h at 80 °C. 3-Thio-butyl iodide (5 g, 25 mmol) was slowly added in a dropwise manner into the solution for 30 min and stirred for 8 h at 80 °C. The resulting mixture was cooled, dried, and concentrated in vacuo to afford a residue which was subjected to recrystallization to yield 4.3 g (67%) of NI−S. Mp 130−132 °C. $^1$H NMR ($CDCl_3$) 2.25 (s, 3H), 2.86 (t, 2H), 4.41 (t, 2H), 7.75 (t, 2H), 8.19 (d, 2H), 8.58 (d, 2H). $^{13}$C NMR ($CDCl_3$) 15.8, 31.9, 39.2, 122.5, 127.1, 128.0, 131.5, 134.0, 134.8, 164.9. FAB-MS for NI−S: found, 272.6 (calcd for [NI−S +1], 271.07).

***N*-(3,9-Dithio-6-oxa-undecyl)-1,8-naphthalimide (NI−SOS).** A solution of 3-oxo-6-thio-octanethiol (2.7 g, 16 mmol) and NaOH (0.7 g, 16 mmol) in 30 mL of MeOH was stirred for 30 min at 50 °C. *N*-(2-bromoethanyl)-1,8-naphthalimide (5 g, 16 mmol) was slowly added in a dropwise manner into the solution for 30 min and stirred for 10 h at 80 °C. The resulting mixture was cooled, dried, and concentrated in vacuo to afford a residue which was subjected to recrystallization to yield 3.4 g (55%) of NI−SOS. Mp 170−171 °C. $^1$H NMR ($CDCl_3$) 1.25 (t, 3H), 2.04 (q, 2H), 2.61 (s, 4H), 2.75 (t, 2H), 3.79 (s, 4H), 4.67 (t, 2H), 7.68 (t, 2H), 8.16 (d, 2H), 8.45 (d, 2H). $^{13}$C NMR ($CDCl_3$) 15.5, 26.1, 29.6, 31.0, 39.3, 39.6, 40.1, 40.7, 41.0, 70.0, 123.0, 127.7, 130.6, 131.4, 134.9, 164.9. FAB-MS for NI−SOS: found, 392.1 (calcd for [NI−SOS +1], 389.11).

**Spectroscopic Measurements.** Time-resolved fluorescence spectra were measured by the single photon counting method,[22] using a streakscope (Hamamatsu Photonics, C4334−01) equipped with a polychromator (Acton Research, SpectraPro150). An ultrashort laser pulse was generated with a Ti:sapphire laser (Spectra-Physics, Tsunami 3941-M1BB, fwhm 100 fs) pumped with a diode-pumped solid-state laser (Spectra-Physics, Millennia VIIIs). For excitation of the sample, the output of the Ti:sapphire laser was converted to THG (300 nm) with a harmonic generator (Spectra-Physics, GWU-23FL). The instrument response function was also determined by measuring the scattered laser light to analyze a temporal profile. This method gives a time resolution of about 50 ps after the deconvolution procedure. The temporal emission profiles were well fitted into a single- or double-exponential function. The residuals were less than 1.1 for each system.

Steady-state UV−vis absorption spectra were recorded with a UV−vis spectrophotometer (Shimadzu, UV-3100) at room temperature. Fluorescence spectra were measured using a Hitachi 850 fluorophotometer. Fluorescence quantum yields were measured using standard fluorescence dyes with known quantum yields (anthracene ($\phi_f$ = 0.30) in toluene for SW, perylene ($\phi_f$ = 0.87) in ethanol for MW, and rhodamine B ($\phi_f$ = 0.65) in ethanol for LW).[23] Fluorescence quantum yields were calculated from the area of each species separated by the curve fitting method.

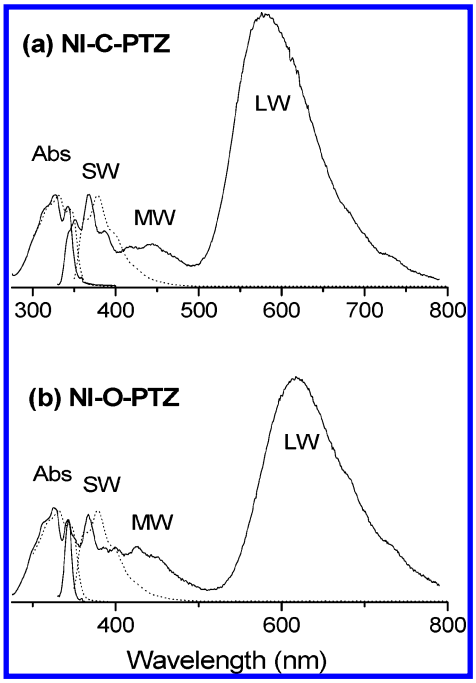


**Figure 1.** Steady-state absorption and fluorescence spectra of NI−C−PTZ (a) and NI−O−PTZ (b) in *n*-hexane (solid line) and in acetonitrile (dotted line). The excitation wavelength was 310 nm. SW, MW, and LW denote the fluorescence bands in regions of shorter, middle, and longer wavelengths, respectively.

## 3. Results and Discussion

**Steady-State Absorption and Emission Properties.** The absorption and fluorescence spectra of NI−C−PTZ and NI−O−PTZ in *n*-hexane are shown in Figure 1. The absorption spectra of reference NI molecules are identical to those of NI-L-PTZ dyads, since the PTZ and L moieties have absorption in a shorter wavelength than 320 nm, indicating that there is no ground-state interaction between the NI and PTZ and L moieties as in acetonitrile (Table 1).

However, the fluorescence spectra of NI−L−PTZ dyads in *n*-hexane showed three bands in the shorter (∼365 nm), middle (∼450 nm), and longer (∼600 nm) wavelengths (SW, MW, and LW, respectively), in contrast to the spectrum in acetonitrile in which only SW emission was observed, implying that the excited-state conformational interaction takes place in the nonpolar solvent. The SW emission maxima of NI−C−PTZ and NI−O−PTZ shifted to 380 nm in acetonitrile (Figure 1). Such a bathochromic shift in polar solvents and the decrease of vibronic shoulders in nonpolar solvents such as *n*-hexane are well-known for the fluorescence spectra.[24] SW fluorescence originated from the NI moiety in the singlet excited state ($^1$NI*). The SW fluorescence quantum yields ($\phi_f^{SW}$) of NI−C−PTZ and NI−O−PTZ were found to be $1.3 \times 10^{-4}$ and $2.5 \times 10^{-4}$ in *n*-hexane (Table 2), and $1.1 \times 10^{-2}$ and $1.6 \times 10^{-2}$ in acetonitrile, respectively. The $\phi_f^{SW}$ values of NI derivatives can be rationalized in terms of two closely spaced upper excited triplet ($n,\pi^*,T_2$) and excited singlet ($\pi,\pi^*,S_1$) states. A close proximity of two states can alter the photophysical behavior of systems containing both nonbonding and $\pi$-electron is well documented in the literature.[24] The relative ordering and spacing

**TABLE 1: Absorption and Fluorescence Maxima in *n*-hexane and Acetonitrile and Dipole Moments of NI Derivatives**

| | absorption (nm) | | fluorescence[a] (nm) in *n*-hexane | | | |
|---|---|---|---|---|---|---|
| NI derivatives | in *n*-hexane | in acetonitrile | SW | MW | LW | dipole moment (Debye) |
| NI−C−PTZ | 327, 342 | 331, 345 | 367 | ∼445 | 582 | 6.0 |
| NI−O−PTZ | 327, 342 | 331, 345 | 366 | ∼449 | 618 | 4.9 |
| NI−C1 | 327, 342 | 330, 344 | 367 | ∼440 | | 4.1 |
| NI−C7 | 328, 343 | 331, 345 | 368 | ∼440 | | 4.0 |
| NI−O1 | 327, 342 | 331, 344 | 369 | ∼440 | | 4.6 |
| NI−O3 | 329, 343 | 332, 345 | 369 | ∼440 | | 4.7 |
| NI−S | 327, 343 | 332, 345 | 366 | 438 | | 5.4 |
| NI−SOS | 325, 341 | 332, 345 | 367 | 461 | | 6.1 |

[a] SW, MW, and LW denote the fluorescence bands in regions of shorter, middle, and longer wavelengths, respectively.

**TABLE 2: Fluorescence Lifetimes ($\tau_f$) and Fluorescence Quantum Yields ($\Phi_f$) of $^1$NI* in *n*-hexane[a]**

| | 380 nm (SW) | | 480 nm (MW) | | 600 nm (LW) | |
|---|---|---|---|---|---|---|
| | $\tau_f$ (ps)[c] | $\Phi_f$ ( $\times 10^{-3}$) | $\tau_f$ (ns) | $\Phi_f$ ( $\times 10^{-3}$) | $\tau_f$ (ns) | $\Phi_f$ ( $\times 10^{-3}$) |
| NI−C−PTZ | <50 | 0.13 | 1.47 | 0.08 | 5.35 (2.38)[b] | 4.05 |
| NI−O−PTZ | <50 | 0.25 | 1.87 | 0.04 | 5.22 (1.28)[b] | 4.66 |
| NI−C1 | <50 | 1.79 | 1.16 | 0.06 | | |
| NI−C7 | <50 | 1.90 | 1.70 | 0.11 | | |
| NI−O | <50 | 2.78 | 1.29 | 0.06 | | |
| NI−O3 | <50 | 2.86 | 1.43 | 0.09 | | |
| NI−S | <50 | 0.61 | 8.67 | 0.40 | | |
| NI−SOS | <50 | 2.74 | 15.7 | 2.30 | | |

[a] MW and LW denote the fluorescence bands in the regions of middle and longer wavelengths, respectively. [b] Values in parentheses indicate those measured in toluene. [c] For all NI, the trace amount (<2%) of the longer component is observed. These decay time constants are in the range of 1.1−3 ns, respectively.

between these states are altered with the change of the polarity. In the present case, as the solvent polarity increases, the $S_1$ state shifts to a lower energy, whereas the $T_2$ state shifts to a higher energy. In nonpolar solvents, when two states are in close proximity, the intersystem crossing of $S_1 \rightarrow T_2$ is an efficient process.[24] We suggest that this is not only a reason for a low $\phi_f^{SW}$ value in *n*-hexane but also due to the formation of the dimer in the excited state. Therefore, the $\phi_f^{SW}$ values of NI−C−PTZ and NI−O−PTZ in *n*-hexane are smaller by a factor of nearly 100 than those in acetonitrile. Thus, their SW fluorescence lifetimes in *n*-hexane were also observed to be shorter than the limitation of the employed instrument and could not be precisely measured. On the basis of the instrumental limitation, we can conclude that the SW fluorescence lifetimes of all NI derivatives are expected to be shorter than 50 ps (Table 2).

As mentioned above, the emission spectra of NI−C−PTZ and NI−O−PTZ in *n*-hexane present two extra emission bands; a low intensity MW emission around 450 nm and an intense LW emission around 600 nm. These MW and LW emission bands were not observed in acetonitrile. For NI−C−PTZ and NI−O−PTZ dyads in *n*-hexane, the maxima of broad LW emission were found to be 580 and 600 nm, respectively. The LW emission of NI−C−PTZ and NI−O−PTZ was also observed in other nonpolar solvents such as toluene, but their LW emission intensities measured in toluene are lower than those in *n*-hexane. It is also important to note that the LW emission was not observed in the cases of reference NI molecules. Since the LW emission is not observed from the reference NI molecules (Figure 2), the LW emission can be assigned to the intramolecular exciplex originating from the interaction between the excited NI and PTZ moieties. We can reasonably exclude the intermolecular exciplex formation, because the solubility is very low in *n*-hexane. The maximum optical density on NIs saturated solution is less than 0.3 in a cell with a 1 cm optical path at the absorption maximum of 327 nm; in these cases, the concentration of NI in *n*-hexane solution is assumed to be $<2.5 \times 10^{-5}$ M which can be determined by the previously reported $\epsilon$ value (12 600 $M^{-1}$ $cm^{-1}$ at 330 nm) in cyclohexane.[24] The ratio of relative intensity between SW and LW emissions did not change by reducing the concentration ∼10 times, thus, no concentration effect was observed.

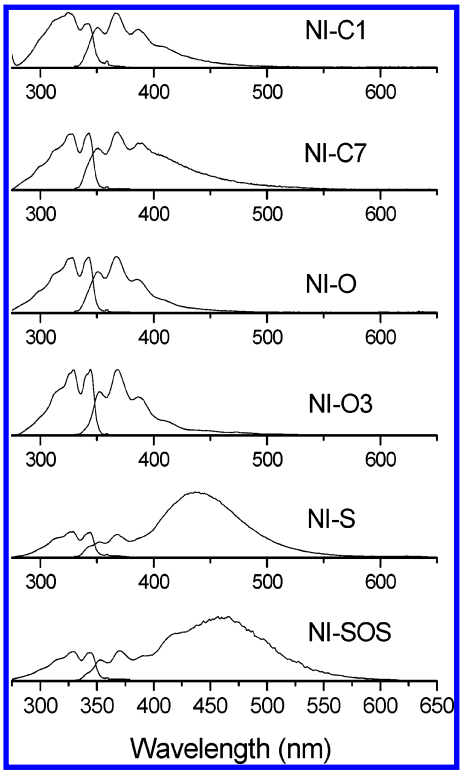


**Figure 2.** Absorption and fluorescence spectra of reference NI molecules in *n*-hexane. The excitation wavelength was 310 nm.

It can be easily referred that the NI and PTZ moieties of NI−L−PTZ dyads are originally separated in polar solvents, but they seem to easily associate in nonpolar solvents. Furthermore, we could not observe any other evidence on the exciplex

formation in acetonitrile, even at high concentration, because polar solvents prevent the exciplex formation between NI and PTZ moieties connected by flexible linkers. Since NI and PTZ are polar in nature, they are separated by polar solvent molecules while they are easily associated in nonpolar solvents as observed by Mataga et al.[9] Intramolecular exciplex formation by associated interaction between excited NI and PTZ moieties can be expected to be probable in nonpolar solvents but not in polar solvents.

It is noteworthy that the MW emissions of NI−C−PTZ and NI−O−PTZ were observed around 450 nm (Figure 1). In the cases of reference NI molecules, the MW emissions were also observed around 470 nm in *n*-hexane (Figure 2). Barros et al.[25] previously investigated the excimer $^1$(NI/NI)* emissions around 480 nm from 1,8-*N*-propyldinaphthalimide and 1,8-*N*-butyldinaphthalimide. Therefore, this band could result from an intermolecular excimer $^1$(NI/NI)*. This excimer emission was not observed in acetonitrile. In nonpolar solvent such as *n*-hexane, NI derivatives can easily form the excimers by the associative interaction between excited NI and ground-state NI molecules which have polar character. Actually, we calculated the dipole moments of NI derivatives to be 4−6 D using the semiempirical method (PM3). Especially, NI−S and NI−SOS showed the high dipole moment values of 5.4−6.1 D. Consequently, the steady-state emission spectra of NI−S and NI−SOS showed intense MW emission by excimer formation. Moreover, NI is a flat molecule which favors the face-to-face excimer in *n*-hexane. These excimers seem to be easily dissociated in polar solvent such as acetonitrile. The MW emission intensities of other NI derivatives were relatively weak compared with those of NI−S or NI−SOS (Table 2). The reason for the high intensities of NI−S and NI−SOS is not presently well understood. The lifetime of MW emission NI−S and NI−SOS is relatively longer than those of other NI derivatives (Table 2). This implies that associations of NI−S and NI−SOS in the excited state are stronger than others.

The MW emission of NI−SOS showed the strong concentration effect. The ratio of MW/SW emission increased according to increasing concentration (Figure S1 in the Supporting Information). This result is a strong evidence for the assignment that the MW emission correlates to the intermolecular interaction (intermolecular excimer formation). Unfortunately, it is hard to measure the concentration effect on other NI derivatives, because of the low quantum yields and poor solubilities of the other NI derivatives.

**Time-Resolved Emission Spectral Properties**. Figure 3 is the time-resolved fluorescence spectra of NI−C−PTZ and NI−O−PTZ in *n*-hexane with femtosecond pulse excitation. At 30 ps of delay time, the time-resolved emission spectra of NI−C−PTZ and NI−O−PTZ showed an emission around 380 nm, which corresponds to the steady-state SW emission. The decay was obviously very fast and almost within the present instrumental limit (approximately 50 ps). When the time delay was increased, the emission around 380 nm disappeared and the MW at 430 nm and LW around 600 nm appeared consequently. The decay time constants are shown in Table 2. The LW emission lifetimes of NI−C−PTZ and NI−O−PTZ were measured to be 5.35 and 5.22 ns, respectively, and the quantum yields of the LW emission showed similar values (Table 2). It is important to note that the time-resolved LW emission spectra NI−C−PTZ and NI−O−PTZ showed two rise components (Figure 4). The rise time constants of NI−C−PTZ were 88 (major) and 890 (minor) ps, while those of NI−O−PTZ were 60 (major) and 1300 (minor) ps, respectively. Whereas especially for longer

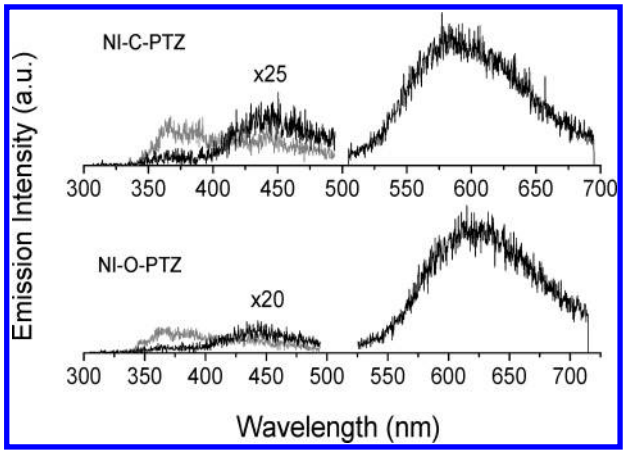


**Figure 3.** Time-resolved fluorescence spectra of NI−C−PTZ and NI−O−PTZ in *n*-hexane; the shorter and longer wavelength fluorescence spectra were measured with delay times of 30 (gray) and 180 (black) ps, respectively, after the laser pulse excitation.

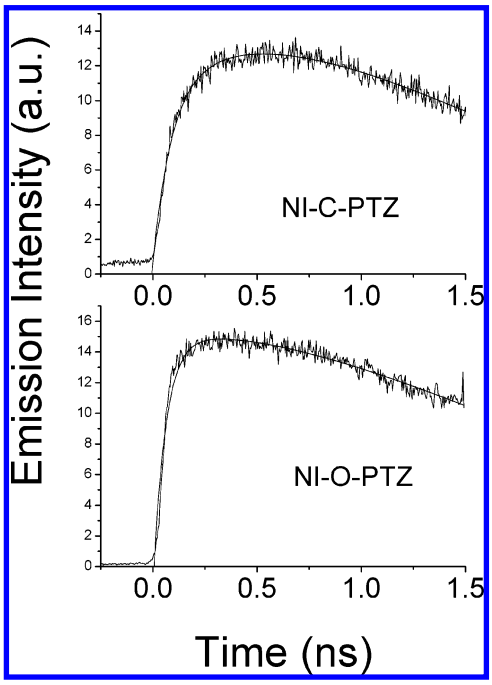


**Figure 4.** LW (excimer) emission rise measured in the wavelength region of 560−675 nm, using the streak camera.

polymethylene linkers a large number of conformations can be envisaged, we have subdivided the origin of the two observed rise components: The fast rise component attributes to an already "folded" but not compact conformation (Scheme 2). The longer rise time constant corresponds to the folding process from an "extended" conformation to a folded one. These rise time constants are not shown to be correlated with the decay time constant of the $S_1$ state, because the main deactivation process of the $S_1$ state is the intersystem crossing process. According to the results reported previously,[25] the rotations of the C−C bonds in longer polymethylene bridges are estimated to have low energy barriers of 2−3 kcal/mol, this allows fast conformational changes within a subnanosecond. Although we should consider the viscosity of solvent, temperature effect, and chain lengths, it may be reasonable to consider that the overall predominant trend for the intramolecular exciplex formation originates from internal rotations around the $-CH_2-$ bonds.

On the other hand, Figure 5 presents the time-resolved fluorescence emission spectra of reference NI molecules in *n*-hexane. For the decay profiles of NI derivatives monitored

**SCHEME 2. Simplified Kinetic Scheme for Excited Inter- (A) and Intramolecular Dimer Formation (B)**

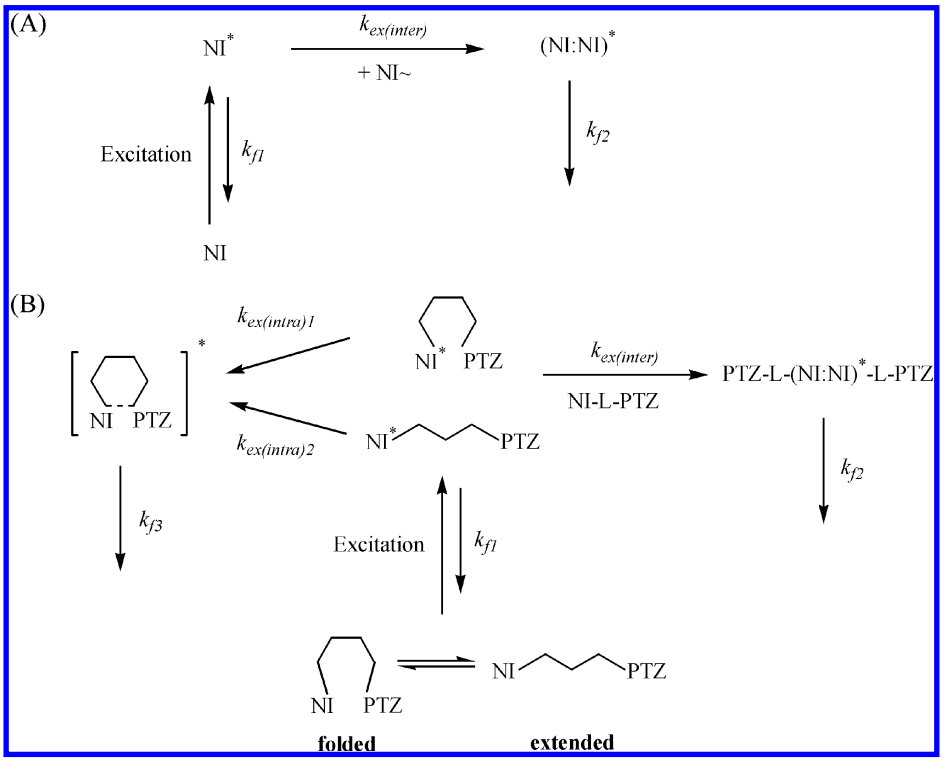


**TABLE 3: Rate Constants ($s^{-1}$) for the Decay of $^1$NI* of NI and NI Dyads in *n*-hexane[a]**

| | $k_{f1}$ | $k_{ex(inter)}$ | $k_{f2}$ | $k_{fex(intra)1}$ | $k_{fex(intra)2}$ | $k_{f3}$ |
|---|---|---|---|---|---|---|
| NI−C−PTZ | $>2 \times 10^{10}$ | | $6.80 \times 10^8$ | $1.15 \times 10^{10}$ | $1.12 \times 10^9$ | $1.87 \times 10^8$ |
| NI−O−PTZ | $>2 \times 10^{10}$ | | $5.35 \times 10^8$ | $1.67 \times 10^{10}$ | $7.69 \times 10^8$ | $1.92 \times 10^8$ |
| NI−C1 | $>2 \times 10^{10}$ | | $8.62 \times 10^8$ | | | |
| NI−C7 | $>2 \times 10^{10}$ | | $5.88 \times 10^8$ | | | |
| NI−O | $>2 \times 10^{10}$ | | $7.75 \times 10^8$ | | | |
| NI−O3 | $>2 \times 10^{10}$ | | $6.99 \times 10^8$ | | | |
| NI−S | $>2 \times 10^{10}$ | | $1.15 \times 10^8$ | | | |
| NI−SOS | $>2 \times 10^{10}$ | | $6.37 \times 10^7$ | | | |

[a] $k_{f1}$, the decay rate constant of the local excited state; $k_{ex(inter)}$, the intermolecular excimer formation rate constant; $k_{f2}$, the decay rate constant of the intermolecular excimer; $k_{fex(intra)1}$, the intramolecular exciplex formation rate constant from the extended dyad conformer; $k_{fex(intra)2}$, the intramolecular exciplex formation rate constant from the folded dyad conformer; and $k_{f3}$, the decay rate constant of the intramolecular exciplex.

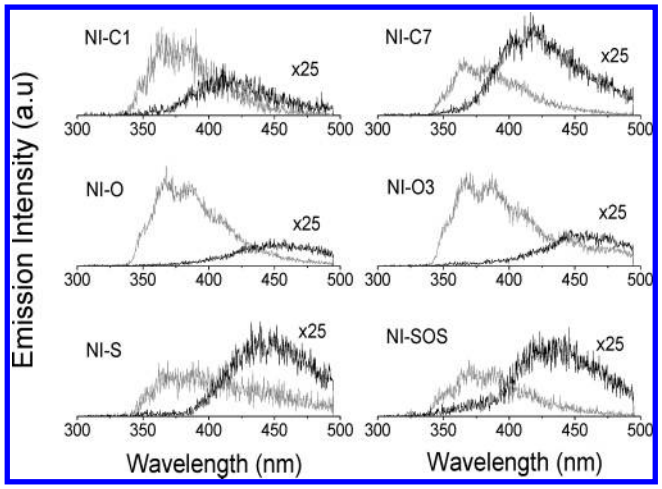


**Figure 5.** Time-resolved emission spectra of reference NI molecules in *n*-hexane; the shorter and middle wavelength fluorescence spectra were measured with delay times of 30 (gray) and 180 (black) ps, respectively, after the laser pulse excitation.

at 380 nm, the SW emission decays were also very fast (<50 ps). In the early time ranges, the SW emission around 380 nm was significantly intense. After this delay in the time scale of 180 ps, the dominant MW emission at 480 nm was clearly observed. The time dependence of the emission at 480 nm on that at 380 nm was not clear, because the SW emission at 380 nm extended to the MW emission region. In other words, the MW emission strongly interfered with the SW emission in the early time range (Figure S2 in Supporting Information). The decay time constants on the MW emission at 480 nm showed the decay time constant in the 1−15 ns range.

In summary, Scheme 2 is proposed to be the mechanism causing the dimer formation in the excited state. The rate constants obtained by exponential fitting of their decay profiles are listed in Table 3. As shown in Scheme 2A, the intermolecular excimer ((NI:NI)*) formation occurred in the NI derivatives in *n*-hexane, exhibiting an MW emission around 470 nm. In NI−L−PTZ dyads, the intermolecular excimer (PTZ−L−(NI:NI)*−L−PTZ) formation occurred as shown in Scheme 2B. Moreover, formation of the intramolecular exciplex between $^1$NI* and PTZ occurred in NI−L−PTZ dyads. The fast rate constants on the exciplex formation are $1.15 \times 10^{10}$ and $1.67 \times 10^{10}$ $s^{-1}$ for NI−C−PTZ and NI−O−PTZ, respectively. The "folded" conformer results in the fast rate constants for the formation of the intramolecular exciplex. In addition, the slower rate constants ($1.12 \times 10^9$ and $7.69 \times 10^8$ $s^{-1}$) for NI−C−PTZ and NI−O−PTZ imply that the intramolecular exciplex formation from the

"extended" conformer corresponds to the conformational change of the linker.

## Conclusions

We found the unique emission band of NI−C−PTZ and NI−O−PTZ around 600 nm in an inert, nonpolar solvent, *n*-hexane. Our finding can be rationalized in terms of a rotation in the flexible chain in $^1$NI*−L−PTZ, resulting in the formation of an intramolecular exciplex between PTZ and $^1$NI*. This process is favored in solvents of relatively low polarity in which the two polar chromophores are close but still electronically independent. Furthermore, all NI molecules have shown the new emission around 470 nm, which can be formed the intermolecular excimer $^1$[NI/NI]*. This study clearly shows that the excited polar solute in a nonpolar solvent environment can easily interact with each other, which resulted in inter- and/or intramolecular excited dimer formation.

**Acknowledgment.** This work has been partly supported by a Grant-in-Aid for Scientific Research (Project 17105005, Priority Area (417), 21st Century COE Research, and others) from the Ministry of Education, Culture, Sports, Science and Technology (MEXT) of the Japanese Government. U.C.Y. acknowledges the Korea Research Foundation (MOEHRD, Basic Research Promotion Fund RO5-2004-000-10557-0) for financial support.

**Supporting Information Available:** Figures showing the emission spectra and temporal profiles of NI−SOS in *n*-hexane monitored at various excitations. This material is available free of charge via the Internet at http://pubs.acs.org.

## References and Notes

(1) Mataga, N.; Kubota, T. *Molecular Interactions and Electronic Spectra*; Marcel Dekker: New York, 1970.

(2) Mataga, N. In *The Exciplex*; Gordon, M., Ware, W. R., Eds.; Academic: New York, 1975; p 113.

(3) Maroncelli, M.; McInnes, J.; Fleming, G. R. *Science* **1989**, *243*, 1674.

(4) *Electron Transfer in Inorganic, Organic and Biological Systems*; Bolton, J. R., Mataga, N., McLendon, G., Eds.; Advances in Chemistry Series; American Chemical Society: Washington, DC, 1991; Vol. 228.

(5) (a) Yoon, U. C.; Mariano, P. S. *Acc. Chem. Res.* **1992**, *25*, 233. (b) Yoon, U. C.; Mariano, P. S. *Acc. Chem. Res.* **2001**, *34*, 523. (c) Yoon, U. C.; Jin, Y. X.; Oh, S. W.; Park, C. H.; Park, J. H.; Campana, J. H.; Cai, X.; Duesler, E. N.; Mariano, P. S. *J. Am. Chem. Soc.* **2003**, *125*, 10664. (d) Yoon, U. C.; Kwon, H. C.; Hyung, T. K.; Choi, K. H.; Mariano, P. S. *J. Am. Chem. Soc.* **2004**, *126*, 1110.

(6) Seischab, M.; Lodenkemper, T.; Stockmann, A.; Schneider, S.; Koeberg, M.; Roest, M R.; Verhoeven, J. W.; Lawson, J. M.; Paddon-Row, M. N. *Phys. Chem. Chem. Phys.* **2000**, *2*, 1889.

(7) Gust, D.; Moor, T. A.; Moor, A. L. *Acc. Chem. Res.* **1993**, *26*, 198.

(8) Wiederrecht, G. P.; Watanabe, S.; Wasielewski, M. R. *Chem. Phys.* **1993**, *176*, 601.

(9) Mataga, N.; Chosrowjan, H.; Taniguchi, *J. Photochem. Photobiol., C* **2005**, *6*, 37.

(10) Vasilescu, M.; Almgren; Angelescu, D. *J. Fluoresc.* **2000**, *10*, 339.

(11) Verhoeven, J. W.; Scherer, T.; Willemse, R. J. *Pure Appl. Chem.* **1993**, *65*, 1717.

(12) Mataga, N.; Murata, Y. *J. Am. Chem. Soc.* **1969**, *91*, 3144.

(13) Masaki, S.; Okada, T.; Mataga, N.; Sakata, Y.; Misumi, S. *Bull. Chem. Soc. Jpn.* **1976**, *19*, 1277.

(14) Mataga, N.; Okada, T.; Masuhara, H.; Nakashima, N.; Sakata, Y.; Misumi, S. *J. Lumin.* **1976**, *12/13*, 159.

(15) Okada, T.; Saito, T.; Mataga, N.; Sakata, Y.; Misumi, S. *Bull. Chem. Soc. Jpn.* **1977**, *50*, 331.

(16) Okada, T.; Migita, M.; Mataga, N.; Sakata Y.; Misumi, S. *J. Am. Chem. Soc.* **1981**, *103*, 4715.

(17) Nakatani, K.; Okada, T.; Mataga, N.; De Schryver, F. C. *Chem. Phys.* **1988**, *121*, 87.

(18) Rogers, J. E.; Weiss, S. J.; Kelly, L. A. *J. Am. Chem. Soc.* **2000**, *122*, 427.

(19) Saito, I.; Takayama, M. *J. Am. Chem. Soc.* **1995**, *117*, 5590.

(20) Armitage, B. *Chem. Rev.* **1998**, *98*, 1171.

(21) Takada, T.; Kawai, K.; Fujitsuka, M.; Majima, T. *PNAS* **2004**, *101*, 14002.

(22) Sakamoto, M.; Cai, X.; Hara, M.; Tojo, S.; Fujitsuka, M.; Majima, T. *J. Phys. Chem. A* **2004**, *108*, 8147.

(23) Murov, S. L.; Carmichael, I.; Hug, G. L. *Handbook of Photochemistry*, 2nd ed.; Marcel Dekker: New York, 1993.

(24) Wintgens, V.; Valet, P.; Kossanyi, J.; Biczok, L.; Demeter, A.; Berces, T. *J. Chem. Soc., Faraday Trans.* **1994**, *90*, 411.

(25) Barros, T. C.; Filho, P. B.; Toscano, V. G.; Politi, M. J. *J. Photochem. Photobiol., A* **1995**, *89*, 141.

(26) Verhoeven, J. W. *Pure Appl. Chem.* **1990**, *62*, 1585.